IOPscience iopscience.iop.org

Home Search Collections Journals About Contact us My IOPscience

The effects of point-like pinning in a vortex lattice

This article has been downloaded from IOPscience. Please scroll down to see the full text article.

1996 J. Phys.: Condens. Matter 8 6747

(http://iopscience.iop.org/0953-8984/8/36/025)

View the table of contents for this issue, or go to the journal homepage for more

Download details:
IP Address: 171.66.16.206
The article was downloaded on 13/05/2010 at 18:38

Please note that terms and conditions apply.

J. Phys.: Condens. Matter **8** (1996) 6747–6758. Printed in the UK

The effects of point-like pinning in a vortex lattice

Sahin Aktas

Marmara University, Faculty of Art and Science, Department of Physics, Istanbul, Turkey

Received 5 October 1995, in final form 12 April 1996

Abstract. The effect of a point-like pinning centre in a vortex lattice formed in a sample size of the order of microns is investigated by using the force calculation method. The possible types of interaction between the pinning centre and the surrounding vortices are simulated to see the nature and extent of distortions in the vortex lattice. The primary results suggests a critical parameter for a phase transition from a long-range orderly state to a disorganized vortex state for a sample grain size of the order of microns. The effect of pinning is found to increase for higher applied fields.

1. Introduction

Right after the discovery of the new type of high-temperature superconductors, there was great excitement about its technological impact. These new superconductors are type II and allow magnetic flux to penetrate as quantized magnetic vortices carrying a quantum of flux ϕ_0. When these superconductors carry an applied current, the Lorentzian type of interaction between the applied current and the vortices causes the vortices to move, which in turn creates a resistive loss, resulting in a reduction in the current-carrying capacity (critical current J_c) of the superconducting material. Therefore, the vortices must be strained to be immobile in order to increase J_c. The various defects in the material already prevent the vortices from moving freely since the vortices are pinned down and do not move at all until a greater force acts upon on them to free the vortices from pinning.

There has been extensive study of the nature and effects of pinning to increase the current-carrying capacity that is very important for the technological uses of superconductors. The Ginzburg–Landau free energy has been used in a number of published simulations [1–3].

In the present article, the nature and the scale of possible interactions between a pinning centre and the surrounding vortices will be studied by the force calculation method instead of the free-energy method so that the collective behaviour of the vortex lattice under a pinning force will be studied.

2. The Lorentz force between vortices

A vortex consists of a normal region called the core with a radius equal to the coherence length, and a region of circulating screening current $\boldsymbol{J}$ with a radius equal to the penetration depth λ. When the density of vortices is so low that their average separation is much larger than λ, the forces between them can easily be calculated through the Lorentz force expression $\boldsymbol{F} = \boldsymbol{J} \times \boldsymbol{\phi_0}$, since the currents of one vortex can be assumed to be uniform over the region

0953-8984/96/366747+12$19.50 © 1996 IOP Publishing Ltd

of the other vortex. When the density of vortices increases to a point where the average distance between them is comparable with λ, then the force can no longer be calculated in this simple way, but the integral of $\boldsymbol{J} \times \boldsymbol{B}$ must be evaluated.

The London equations can be used to treat the vortices up to the density where they have the separation $D = 5.4\xi$ [4, 5] which corresponds to an applied field of about $\frac{1}{4}H_{c2}$ for $\kappa(\lambda/\xi) = 100$. This approach is appropriate especially for high-κ cases where the core region can be treated as point like compared with the penetration depth λ. The field and the current distribution of a single vortex are obtained by solving the London equations in an isotropic plane as given by [6]

$$B_z(r) = \frac{\phi_0}{2\pi\lambda^2} K_0(r) \tag{1}$$

$$J_\theta(r) = \frac{\phi_0}{2\pi\lambda^3} K_1(r) \tag{2}$$

where $K_0(r)$ and $K_1(r)$ are the zeroth- and first-order modified Bessel functions, respectively, and r is normalized with λ. The vortices are assumed to be aligned with the symmetry axis of the axially symmetric superconductor. Using the field and the current distributions given by equations (1) and (2), the Lorentz force between two vortices was calculated and it was used to simulate the formation of a vortex lattice in a previous study by Aktas *et al* [7]. In the present article, the same method will be used to deal with vortex–vortex interactions in the simulations.

3. Pinning force

The best part of a computer simulation of a physical problem is that the problem can really be approximated to simpler steps without involving the complexity of the problem. In the simulations, vortices were treated as classical particles with a repulsive interaction, and pinning centres were approximated by the centres of attractive potentials with the interaction ranges of λ. The hard-core part of the potential is neglected. This corresponds to assuming that the Ginzburg–Landau constant κ is large. The pinning has been treated in this way in recent studies represented by [8, 9]. Two different types of potential model has been tried to represent different pinning mechanisms. The possible outcome for each case has been simulated in a vortex lattice formed by 800 vortices. The exact method of simulating the formation of a vortex lattice has already been given in the article by Aktas *et al* [7]; here the only addition to that simulation is the addition of the pinning sites to the scheme to see the resulting effects on the lattice structure, and the size and the number of vortices have doubled. The pinning–vortex interaction $\boldsymbol{F}_p$ can in general be represented as

$$\boldsymbol{F}_p = Cf(r)\hat{\boldsymbol{r}} \tag{3}$$

where C is related to the strength of the interaction such that $C = 1$ means a normalization to the scale of vortex–vortex interaction that the peak value of the vortex–vortex repulsive force has been calculated as being approximately at the order of 10^{-10} N m^{-1} for the case when $\lambda = 1000$ Å, and the sign of C determines whether it is an attractive or repulsive interaction (negative C means an attractive interaction). The function $f(r)$ represents the r dependence of the interaction which will be studied. The vector $\boldsymbol{r}$ is the directional vector towards the vortex along the line which connects the pinning and the vortex.

The first choice for $f(r)$ is an exponential dependence since the vortex–vortex interaction has an exponential dependence for $r \gg \lambda$. On the other hand some other mechanism should also be tried like $1/(\omega^2 + r^2)$ to include a possible Coulombic interaction.

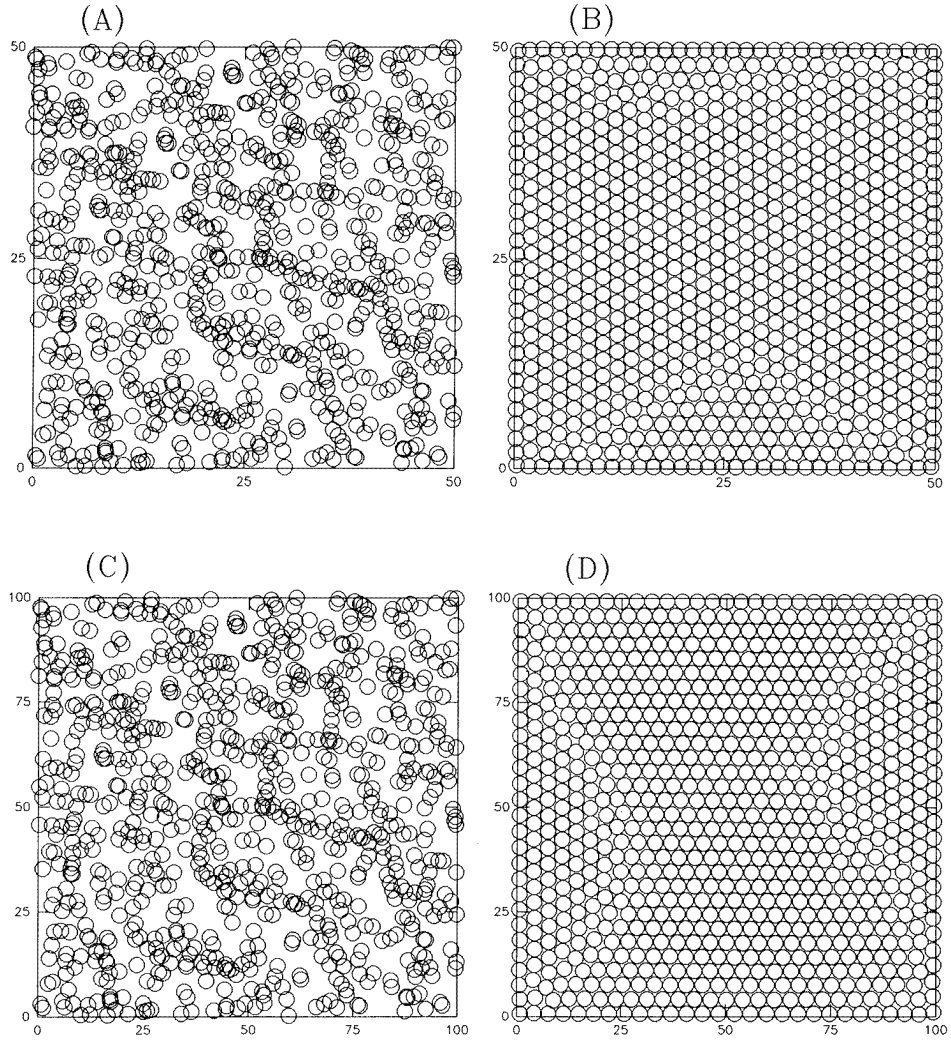

Figure 1. (a) The initial configuration of randomly located vortices. (b) After 2000 steps, the resultant configuration of vortices without a pinning. Here the size of the sample is $50\lambda \times 50\lambda$ square, and the number of vortices is 800. The radius of the circles in the figure that represent vortices are scaled to λ. (c) and (d) same as (a) and (b) except for a sample size of $100\lambda \times 100\lambda$.

4. Simulations

The pinning centre is assumed to be immobile and positioned at the centre of the vortex population in two different ways.

(a) The pinning centre is placed at the beginning phase of the vortex lattice simulation from initially randomly placed vortices.

(b) The pinning centre is added in a later phase such that an orderly vortex lattice had already been formed in the absence of any pinning centre.

The simulations were performed for sample sizes of $50\lambda \times 50\lambda$, and $100\lambda \times 100\lambda$ to

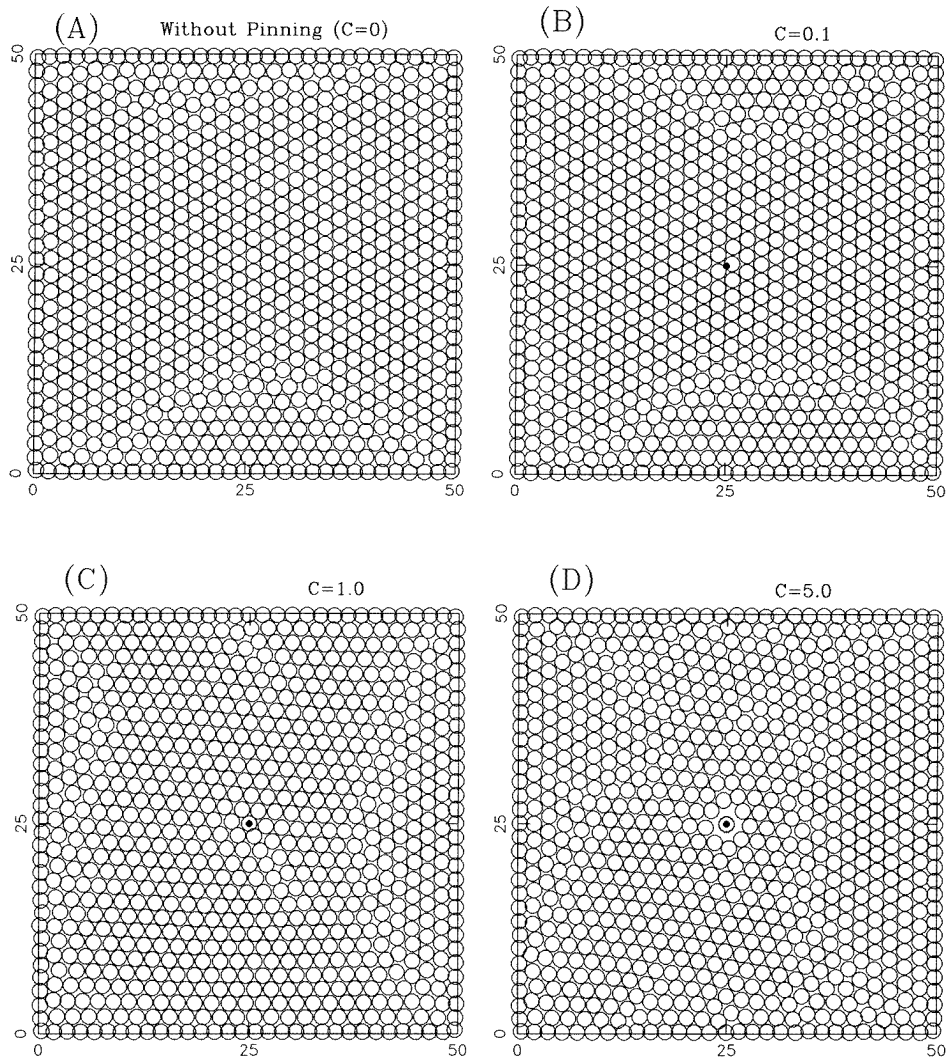

Figure 2. Effect of the pinning for a sample size of 50×50. (a) Vortex configuration without the pinning. (b) With the pinning of the interaction strength $C = 0.1$. The pinning centre is marked by the full circle at the centre of the sample. There is almost no effect of the pinning. (c) The case with $C = 1$, where the pinning seems to change the symmetry but vortices can still form an orderly state. (d) When $C = 5$, at least two vortices are now centred by the pinning, and the order is broken.

check the size effect. All the lengths throughout the simulations are scaled to unit length λ The vortices are allowed to interact with each other and with the pinning and move a step to reduce the lattice energy. In order to see and compare the effects of different kinds of pinning, the same initially randomly positioned vortex population shown in figure 1 is used to start the simulations in all the different cases. Figures 1(b) and 1(d) show the resultant hexagonal vortex states that are formed in the absence of any imperfections, without any pinning interactions. Here, the vortices form the main domain which covers most of the vortex population. At the edges of the sample the density of the vortices increases, and

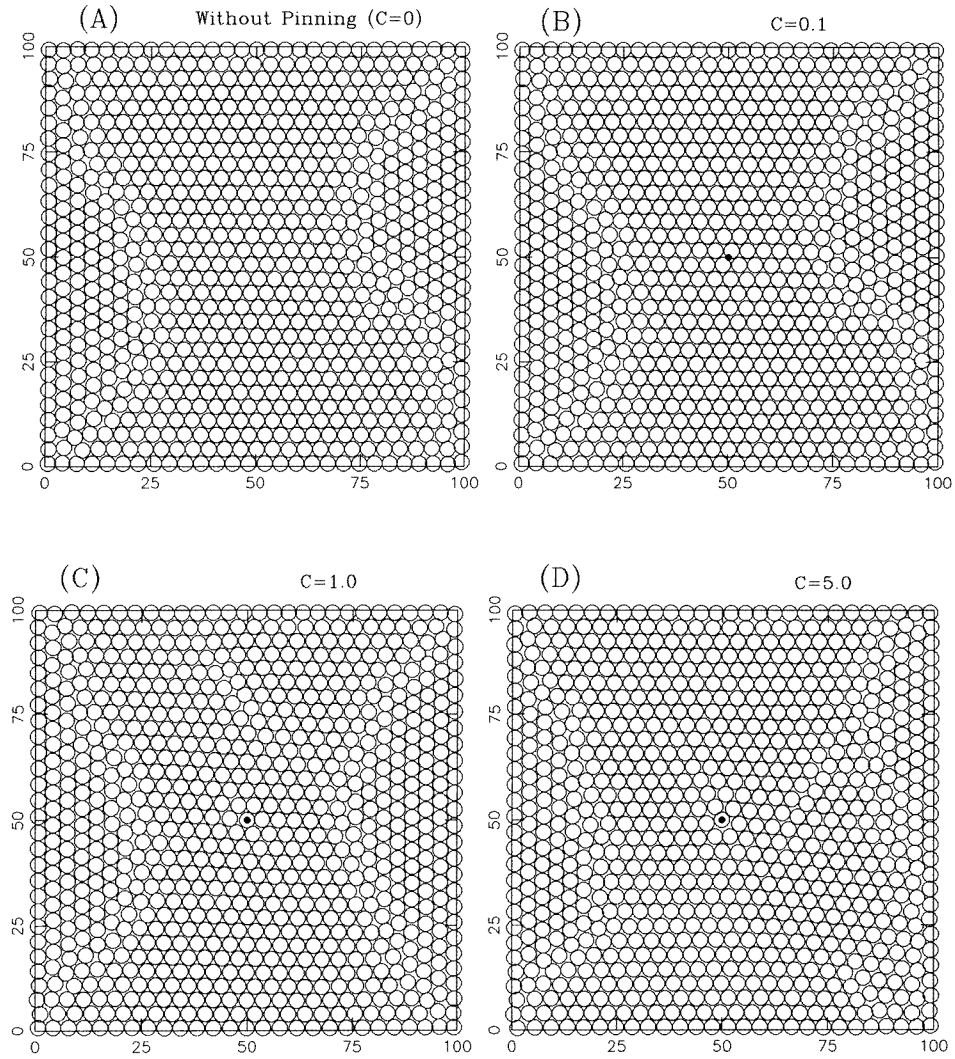

Figure 3. Same simulations represented by figure 1, except for a larger sample size of 100×100. Here pinning seems weaker so that it can barely break the symmetry for $C = 5$.

the vortices are aligned with the edges to comply with the boundary conditions due to the outside applied field. The effect of pinning will be studied by comparing this undisturbed pattern with the cases including pinning.

4.1. The case for $f(r) = Cexp^{(-r)}$

The pinning–vortex interaction is assumed to decrease exponentially with the scale of the normalized distance r. Figure 2 shows the resultant configurations of vortex populations with a pinning of the same type but of different strengths for a sample size of $50\lambda \times 50\lambda$. Figure 3 is same as figure 2 but for a sample size of $100\lambda \times 100\lambda$. Figures 2(b) and 3(b) give the case where C is 0.1. Here the existence of the pinning centre is almost unnoticeable in both cases.

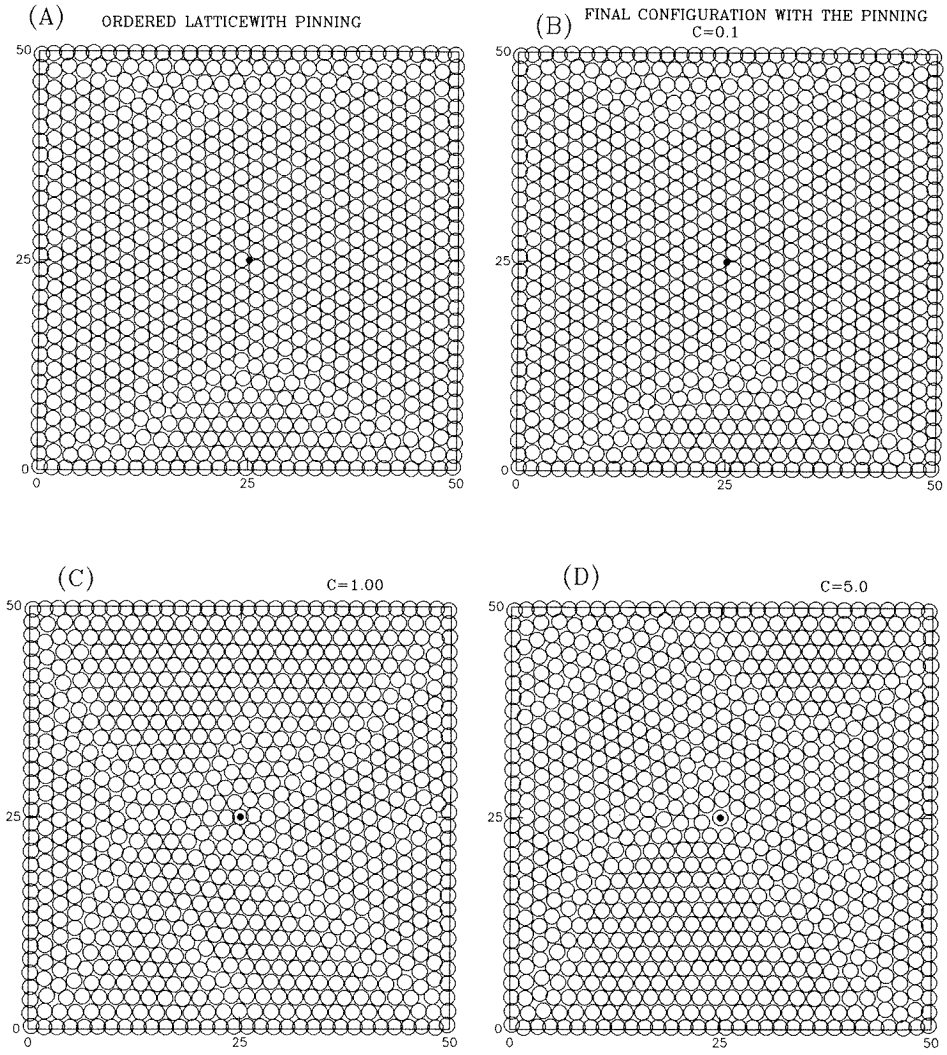

Figure 4. The case when the pinning centres were introduced after the vortex lattice is formed for a sample size of 50×50. (a) The configuration of vortices at the moment when the pinning centre is placed at the centre of the sample. (b) After the vortices were relaxed to resettle with the pinning. Here too, with $C = 0.1$, pinning is not strong enough to have an impact. (c) Pinning with $C = 1$ reshuffles the vortices. (d) With $C = 5$, pinning is strong enough to destroy the vortex lattice.

However, when the strength of the pinning C is raised to 1, there is noticeable distortions in the smaller sample, but the overall vortex configuration still suggests the existence of long-range order within the main domain as seen in figure 2(c), and in figure 3(c). The difference between the two figures suggests that the same pinning centre is more effective in the smaller sample with the same number of vortices in higher fields. In simulations represented by figures 2(d) and 3(d) the pinning strength constant is increased to 5. Here the attractive pinning force succeeds in moving at least two vortices to its location with the

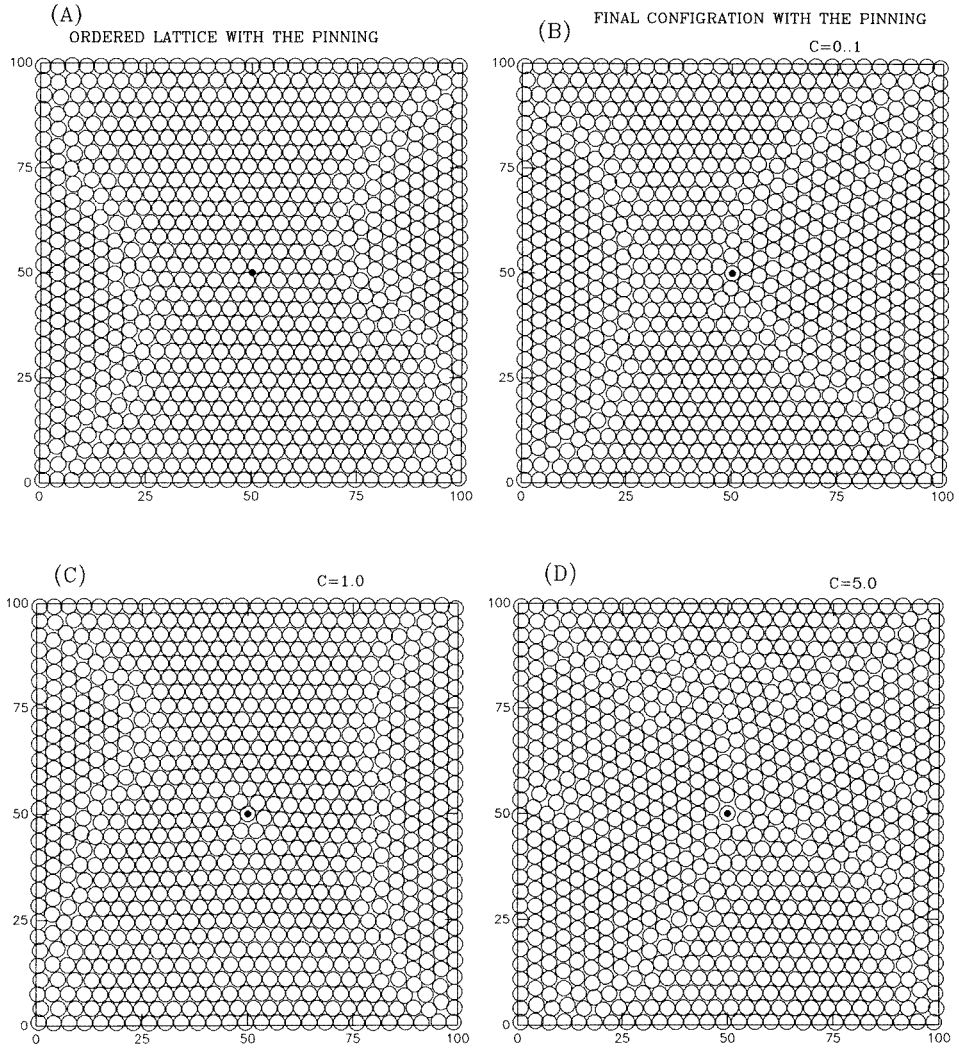

Figure 5. The same type of simulation for a larger size of 100×100. Here too the effect of pinning seems to become weaker compared with figure 4.

result of creating a region of lower density of vortices right around the pinning centre as seen in both cases although to a lesser degree in the larger sample. In the case of the small sample (higher applied field) the whole vortex population is affected by this rather strong attractive pinning so that long-range order cannot be set up by the vortices. This behaviour suggests the occurrence of a phase change in the vortex lattice.

The same simulations are repeated for the cases of inserting pinning centres into the sample after the regular vortex lattice is formed (figure 4). Figures 5 and 6 conclude that the vortex lattice is more stable in cases having pinning centres the whole time instead of at a later time after the lattice is formed.

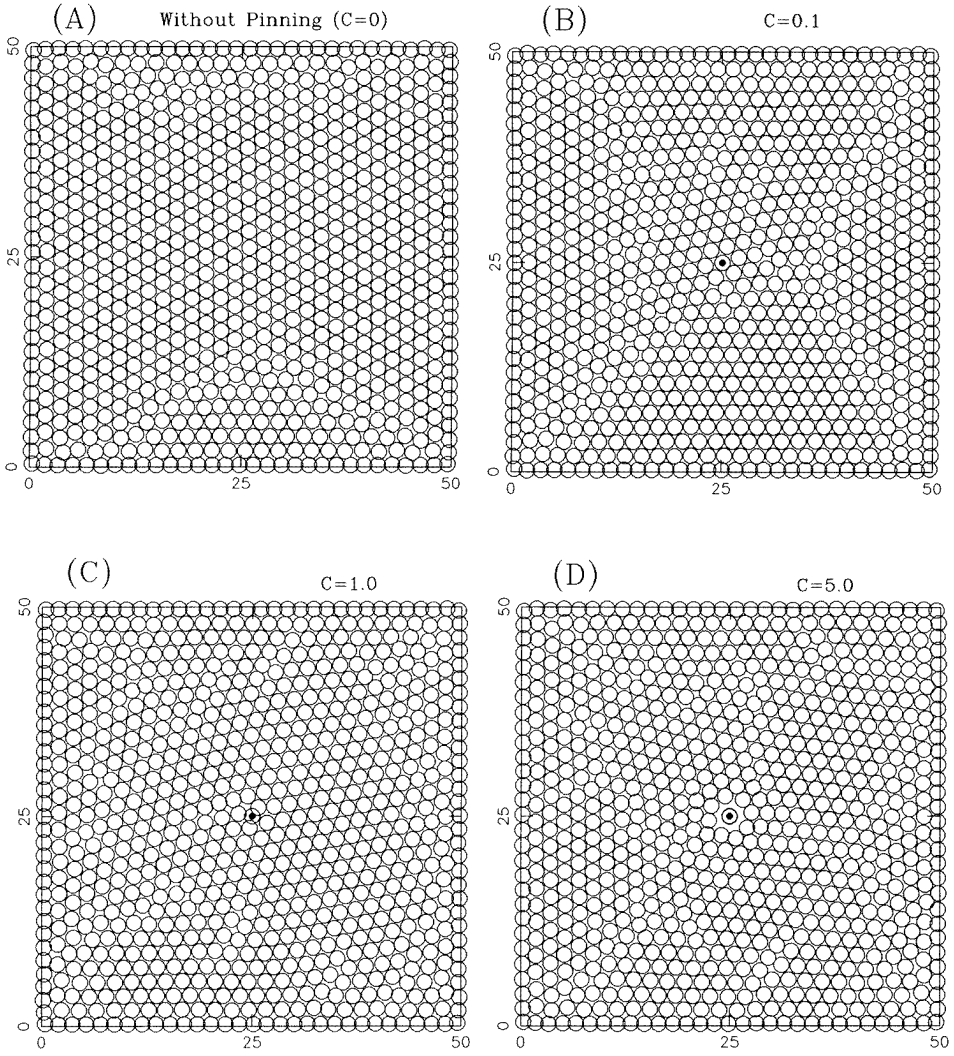

Figure 6. The treatment of pinning represented by a Coulomb-like potential. The sample size is 50×50. (a) Without the pinning. (b) $C = 0.1$ seems to be effective enough to have an impact contrary to the exponential case represented in figure 2(b). (c) With $C = 1$, pinning almost prevents the formation of the vortex lattice. (d) $C = 5$ pinning totally breaks any long-range order.

4.2. The screened Coulomb type $f(r) = C/(\omega^2 + r^2)$

Another possible type of interaction for the pinning can be thought of as Coulomb-like (screened Coulomb). The interaction between localized charge fluctuations and the screening current of vortices can be approximated by this type of interaction. Here $\omega = 1$ is taken for the rest of the paper. Figure 6(b) shows the final vortex configuration for $C = 0.1$ in which the vortices seem to be affected by the existence of the pinning but they still manage to form a distorted hexagonal state. The marked difference from the previous type of pinning is that the Coulombic potential seems to cause a stronger pinning centre. Increasing C to

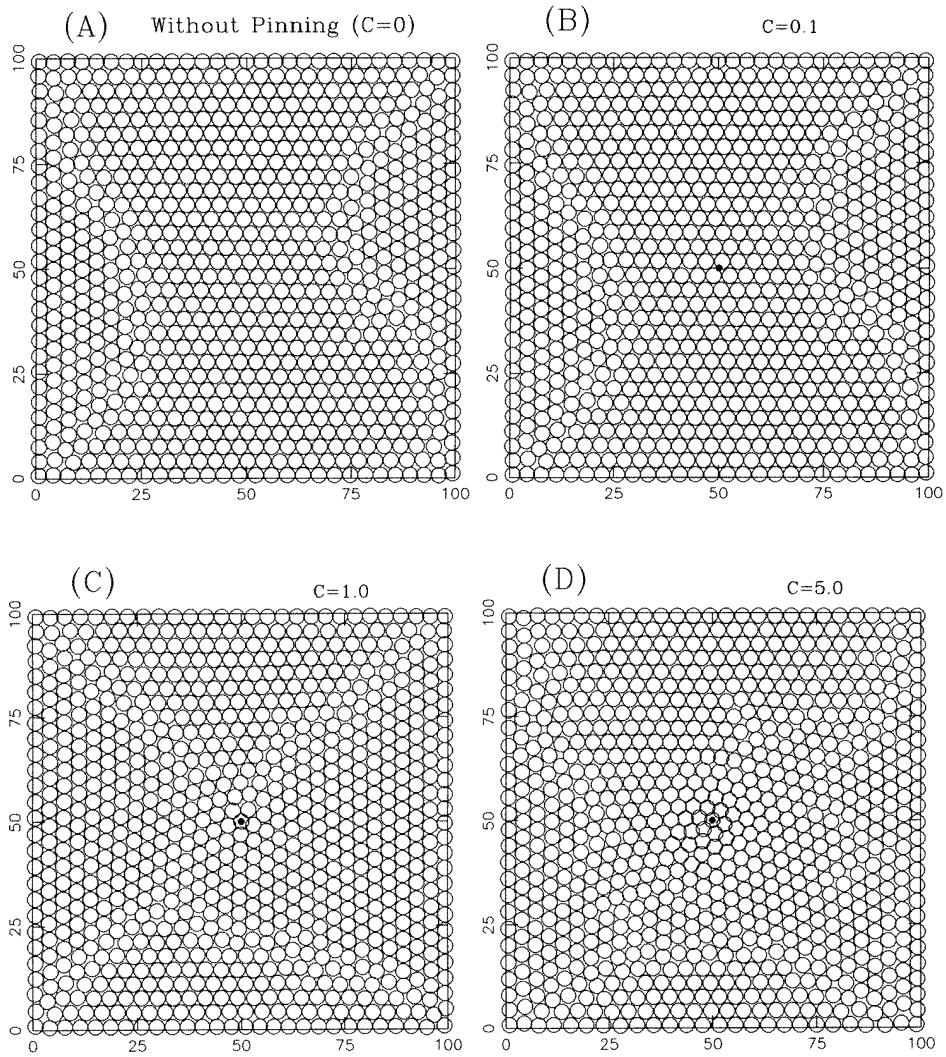

Figure 7. Same as figure 6 except for a larger sample size of 100×100.

1 so as to reach to the same strength with a vortex for $r \approx \lambda$ [7] causes vortices to start to pile up around the proposed pinning centre at the midpoint of the vortex population as seen from figure 6(c). Once the strength parameter C is increased to 5, which is shown by figure 6(d), the pinning destroys the long-range orderly state of vortices by attracting more vortices around the pinning as in the case shown previously in figures 2(d), 3(d), 4(d) and 5(d). The density of vortices around the pinning centre decreases as in the exponential case. The change in the vortex configuration when C is raised from $C = 1$ to $C = 5$ again suggests a kind of phase change as in the exponential case. Increasing the sample size has the same weakening effect for the pinning centre as seen from figures 6(d) and 7(d), thus enforcing the conclusion that pinning centres are more effective at higher applied fields.

The vortex lattice seems to be less stable under the action of pinning represented by a

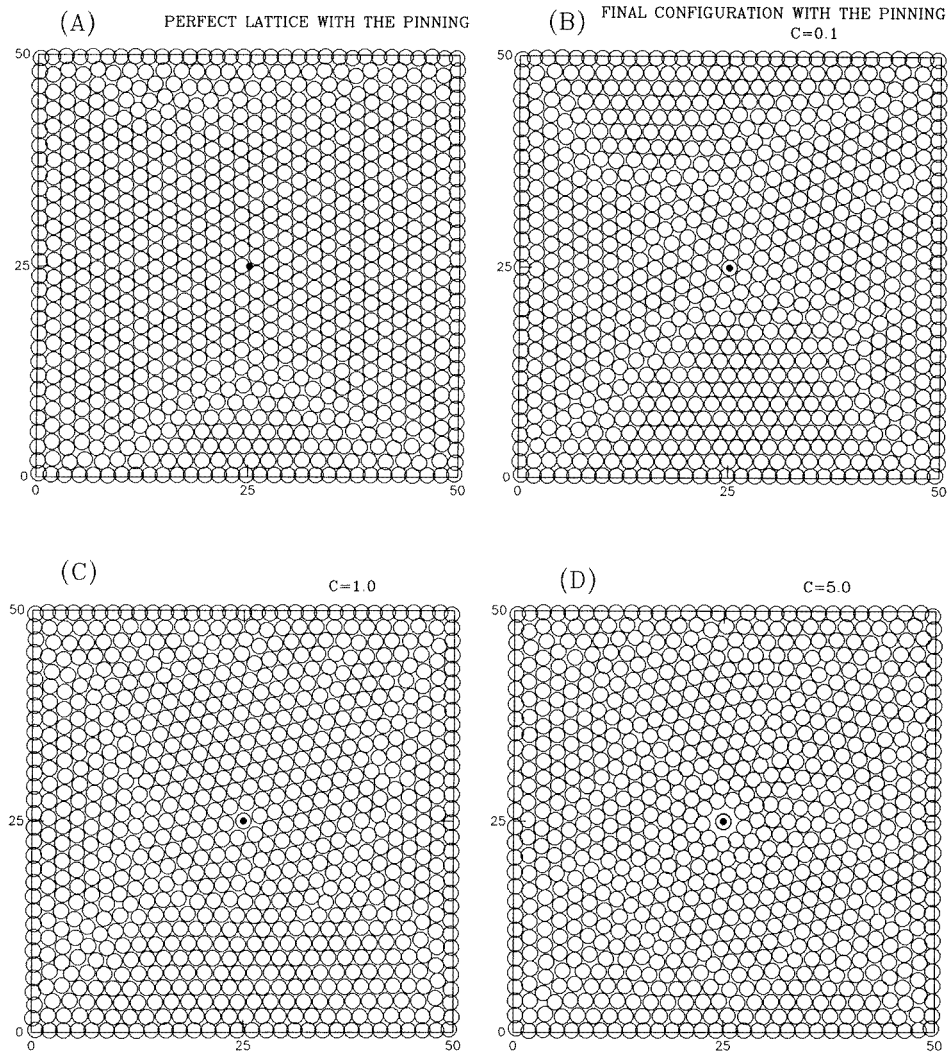

Figure 8. The case for adding the Coulomb-like potential after the vortex lattice is formed for a sample size of 50×50. Compared with the exponential potential, the Coulomb-like potential is more effective owing to a longer interaction range.

Coulombic potential, since a Coulombic potential has a longer range of interaction than an exponential potential with the same interaction constant.

5. Discussion

The stability of the final vortex configurations (as in figures 1(b) and 1(d)) may be a valid issue, since they are dependent on the initial conditions. It appears that a real vortex lattice has more than one equilibrium configuration depending on the initial conditions. This is partly due to the side effect of a finite size sample and the fact that simulations were done without thermal fluctuations at $0\,^{\circ}$C. The vortices seem to lock on to a relative minimum-

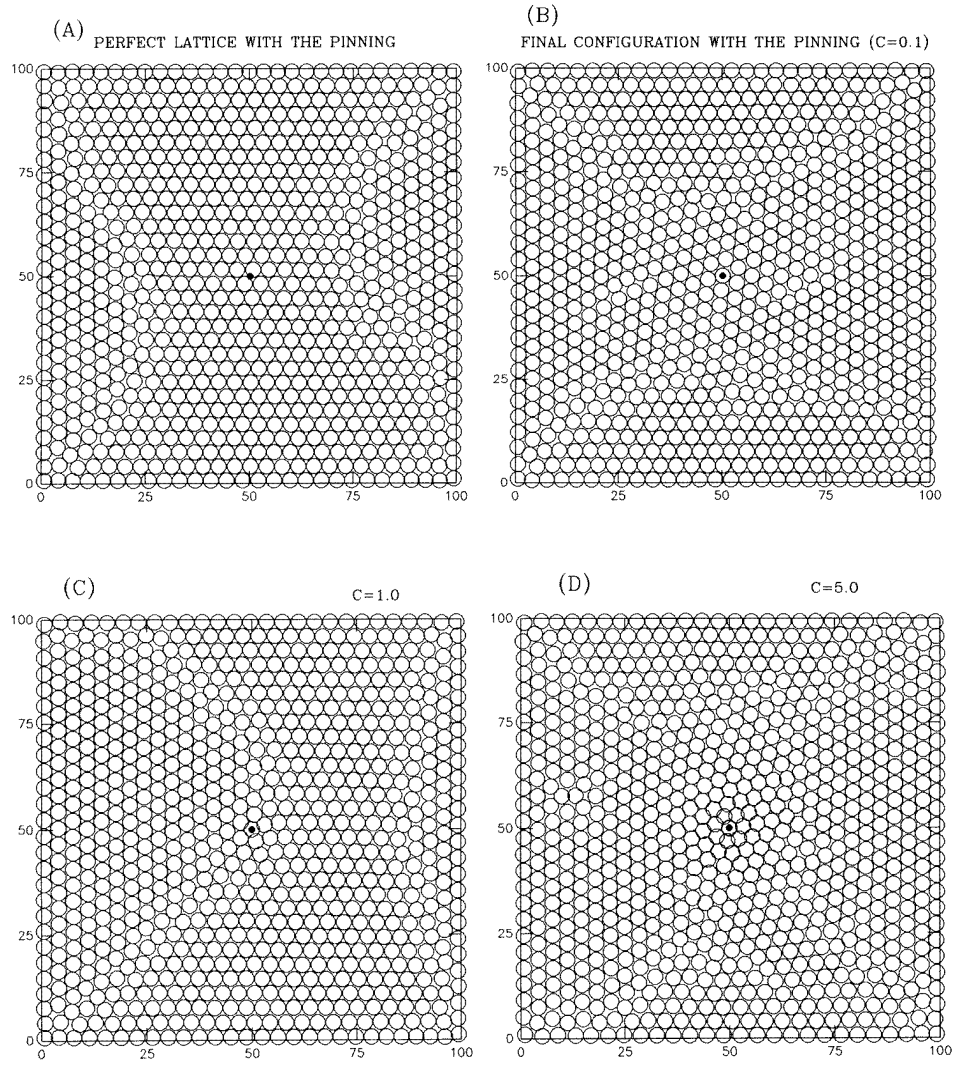

Figure 9. Same as figure 8, except that the size of the sample is 100×100.

energy state. Since these energy levels are stable enough to resist disturbances due to attractive pinning up to a certain extent (the pinning strength constant must be larger than 1 to have an observable effect on vortex configurations as can be seen in figures 2(b), 2(c), 3(b) and 3(c)), this proves the stability of these different vortex configurations. Also the result from the addition of the pinning centre to the vortex lattice as in figure 4 shows that the vortex lattice is stable enough to resist the destabilization caused by the pinning for $C = 0.1$ (compare figures 4(a) and 4(b)).

There seems to have a phase transition depending on the strength of the interaction constant C for the sample sizes represented, no matter what type of pinning that it represents. The transition from a long-range order state to a random state is already expected to occur for a certain C, but it is interesting that it occurs for approximately the same strength

($C = 5$) for the different kinds of interaction for the same sample size that have been investigated. In all cases, the pinning attracts vortices around it, and these vortices in turn create a somewhat isolated region around the pinning. As expected the effect of a single pinning centre diminishes when the sample size increases. Thus the phase transition at $C = 5$ is valid for the specific sample size represented here.

A higher applied field makes a pinning centre more effective, since the number of neighbouring vortices to the pinning centre increases with increasing vortex density. Adding pinning centres to the ordered vortex lattice makes pinning more effective on the vortex lattice as seen by comparing figures 2(c) and 4(c) and figures 3(d) and 5(d).

The field range in which the simulations were made can be found from

$$B_{av} = \frac{n\phi_0}{\text{area}} \tag{4}$$

putting $n = 800$, and the area as $50\lambda \times 50\lambda$ where $\lambda = 1000$ Å; this gives $B_{av} = 0.06$ T and $B_{av} = 0.015$ T for the sample size of $100\lambda \times 100\lambda$. These are reasonable values for the fields expected around a superconducting sample in industrial applications. The size of the sample area used in the simulation is $50\lambda \times 50\lambda = 25\ \mu\text{m}^2$, which is the area of a typical superconducting grain. An experimental study gives a value of around 10^{-6} N m^{-1} for the pinning force in Pb–Bi films [10]. This result is in agreement with the numerical results obtained by our simulations where the scale for the vortex–vortex interaction force for $\lambda = 100$ Å is about 10^{-5} N m^{-1} which is equivalent to $C = 1$ for the pinnings represented in this article.

References

[1] Brandt E H 1983 *J. Low. Temp. Phys.* **531–2** 41
[2] Brandt E H 1983 *J. Low. Temp. Phys.* **531–2** 71
[3] Hwa T, Nelson D R and Vinokur V M 1993 *Phys. Rev.* B **48** 1167
[4] Brandt E H 1972 *Phys. Status Solidi* b **51** 345
[5] Brandt E H 1988 *Phys. Rev.* B **37** 2349
[6] Tinkham M 1985 *Introduction to Superconductivity* (Malahar, FL: Krieger)
[7] Aktas S, Poole C P Jr and Farach H A 1994 *J. Phys.: Condens. Matter* **6** 7373
[8] Richardson R A, Pla O and Nori F 1994 *Phys. Rev. Lett.* **72** 1268
[9] Pla O, Wilkin N K and Jensen H J 1996 *Europhys. Lett.* **33** 297
[10] Hyun O B, Finnemore D K, Schwartzkopf L and Clem J R 1987 *Phys. Rev. Lett.* **58** 599